Close limit from a null point of view: The advanced solution

Manuela Campanelli,[1] Roberto Gómez,[2] Sascha Husa,[1,2] Jeffrey Winicour,[1,2] and Yosef Zlochower[2]

[1]*Max-Planck-Institut für Gravitationsphysik, Albert-Einstein-Institut, 14476 Golm, Germany*
[2]*Department of Physics and Astronomy, University of Pittsburgh, Pittsburgh, Pennsylvania 15260*

We present a characteristic algorithm for computing the perturbation of a Schwarzschild spacetime by means of solving the Teukolsky equation. We implement the algorithm as a characteristic evolution code and apply it to compute the advanced solution to a black hole collision in the close approximation. The code successfully tracks the initial burst and quasinormal decay of a black hole perturbation through 10 orders of magnitude and tracks the final power law decay through an additional 6 orders of magnitude. Determination of the advanced solution, in which ingoing radiation is absorbed by the black hole but no outgoing radiation is emitted, is the first stage of a two stage approach to determining the retarded solution, which provides the close approximation wave form with the physically appropriate boundary condition of no ingoing radiation.

I. INTRODUCTION

In this work, we present the advanced solution for a perturbation of a Schwarzschild background describing the head-on collision of black holes in the close approximation where the merger takes place in the far past. We compute the solution by means of a characteristic evolution of the Weyl tensor, as governed by the Teukolsky equation [1,2]. The advanced solution corresponds to stage I of a new two stage approach to the vacuum binary black hole problem [3]. In subsequent work (stage II), we will use the results of this first stage to compute the physically more relevant retarded solution. This perturbative solution will in turn provide a valuable reference point for the physical understanding of a fully nonlinear treatment of binary black holes being pursued by a similar two stage strategy [4], a computationally feasible problem using an existing characteristic code [5]. The perturbative results also provide a new perspective on the physical picture previously obtained by applying the Cauchy problem to the close approximation [6], especially with regard to global issues which have not yet been explored in the Cauchy formulation.

In the characteristic formulation of this problem, the advanced solution is simpler to compute than the retarded solution because of the global relationship between the null hypersurfaces on which boundary information is known. One of these hypersurfaces is the black hole event horizon $\mathcal{H}^+$ whose perturbation must correspond to the close approximation of a binary black hole. In the retarded problem, the other null hypersurface (in a conformally compactified description) is past null infinity $\mathcal{I}^-$ where the incoming radiation must vanish. Because $\mathcal{H}^+$ and $\mathcal{I}^-$ are disjoint, there is no direct way to use data on those two hypersurfaces to pose a characteristic initial value problem.

However, in the advanced problem, it is at future null infinity that the radiation is required to vanish. Since $\mathcal{H}^+$ and $\mathcal{I}^+$ formally intersect at future time infinity I^+, they can be used to pose a characteristic initial value problem to evolve backward in time and compute the exterior region of spacetime. Potential difficulties in dealing with I^+ are avoided by posing the no outgoing radiation condition on an ingoing null

hypersurface J^+ which approximates $\mathcal{I}^+$ and intersects $\mathcal{H}^+$ at a late time when the perturbation of the black hole has effectively died out. These data on $\mathcal{H}^+$ and J^+ then constitute a standard double-null initial value problem [7–10] for the exterior spacetime, in which ingoing radiation is absorbed by the black hole but there is no outgoing radiation.

This advanced solution provides the radiation incident from $\mathcal{I}^-$. In stage II of the approach, this ingoing radiation will be used to generate a ''source free'' *advanced minus retarded* solution. A purely retarded solution can then be produced by superposition with the stage I solution. Although we do not address stage II in this paper, we will discuss the role of time reflection symmetry in the perturbation equations, which simplifies the technical details in carrying out the superposition. From a time reversed point of view, the stage I solution is equivalent to the retarded solution for a ''head-on'' white hole fission, with the physically relevant boundary conditions that radiation is emitted but that there is no incoming radiation from $\mathcal{I}^-$. It is convenient here to formulate the stage I results in terms of such a white hole fission since the characteristic evolution then takes the standard form of being carried out forward in retarded time.

The close approximation has been extremely useful for testing fully nonlinear Cauchy evolution codes. The results of numerical Cauchy evolution and close-limit perturbative theory are in excellent agreement in the appropriate regime, giving great confidence in both approaches [6,11]. Furthermore, the perturbative approach provides an important tool for the interpretation and physical understanding of those results [12].

Clearly, this vital synergism between numerical and perturbative approaches should also extend to characteristic evolution. However, in all perturbative studies performed to date, the background geometry has either been the Schwarzschild spacetime in standard Schwarzschild coordinates or the Kerr spacetime in Boyer-Lindquist coordinates. These coordinate systems are appropriate for comparison with results from nonlinear Cauchy evolution but, to our knowledge, there does not yet exist a treatment of the close approximation in terms of null coordinates appropriate for the compari-

son with nonlinear characteristic evolution.

This work provides such a framework. The methods and results presented here are expected to have direct bearing on the study of binary black holes presently underway using a fully nonlinear characteristic code. Characteristic evolution has been totally successful in evolving 3-dimensional single black hole spacetimes for effectively infinite times ($t \approx 60\,000M$ in terms of black hole mass) [13]. Although it is not yet known to what extent the characteristic approach can handle the inspiral and merger of binary black holes, it is clear that the limitations are due to difficulties in treating caustics and not due to high nonlinearity.

The characteristic data which has been obtained for the nonlinear description of a binary black hole spacetime generate close approximation data for a perturbative solution. We present here a numerical code to evolve such data as a perturbation of a Schwarzschild spacetime in null coordinates. Fortunately for our purposes, the perturbative formalism due to Teukolsky [2] is amenable to a reasonably straightforward change of background coordinates, as observed in Ref. [14].

The Teukolsky equation is based upon the decomposition of the Einstein equations and Bianchi identities in terms of a conveniently chosen complex null tetrad, as carried out by Newman and Penrose [15] in the early 1960s. The Newman-Penrose formalism allowed Teukolsky to construct a single master wave equation for the perturbations of the Kerr metric in terms of the Weyl curvature components ψ_4 (describing outgoing radiation) or ψ_0 (describing ingoing radiation). The Teukolsky formalism provides a completely gauge invariant spherical harmonic multipole decomposition for both even and odd parity perturbations in terms of radial wave equations. For a Kerr black hole with angular momentum, there is no similar multipole decomposition of metric perturbations in the time domain (as opposed to the frequency domain of Fourier modes). In the non-rotating case, the Teukolsky equation reduces to the so-called Bardeen-Press equation [16].

Since the 1970s the Teukolsky equation for the first order perturbations around a rotating black hole has been Fourier transformed and integrated in the frequency domain for a variety of situations where initial data played no role [17,18]. In order to avoid the important but difficult problem of prescribing physically appropriate initial data for that equation, the computation of gravitational radiation has been restricted to the cases of unbounded particle trajectories or circular motion. The first evolution code to integrate the Teukolsky equation in the time domain, in Boyer-Lindquist coordinates, was recently developed [19] and successfully tested [20]. In order to incorporate initial data representing realistic astrophysical initial data for the late stage of binary black hole coalescence, $3+1$ expressions connecting ψ_4 and its time derivative to Cauchy data (3-metric h_{ij} and extrinsic curvature K_{ij}) satisfying the Hamiltonian and momentum constraints

$$\psi_4 = \psi_4(h_{ij}, K_{ij}), \quad \partial_t \psi_4 = \dot{\psi}_4(h_{ij}, K_{ij}),$$

have been worked out explicitly [21,20,22,23].

In Sec. II, we specify a null background tetrad suitable to reexpress the Teukolsky equations for ψ_0 and ψ_4 in null coordinates appropriate for characteristic evolution. We also discuss various global aspects of these equations which are important for numerical evolution. In Sec. III, we discuss data for the Teukolsky equation. We present null data for linearized Robinson-Trautman solutions, which provide an analytic check on numerical accuracy, and null data for the close approximation to a white hole fission. In Sec. IV, we discuss the numerical algorithm used to carry out the characteristic evolution. The properties of the close approximation wave forms, are presented in Sec. V.

Notation and conventions: We use a metric of signature $(-+++)$ and a null tetrad with normalization $l^a n_a = -m^a \bar{m}_a = -1$, so that $g_{ab} = 2(m_{(a}\bar{m}_{b)} - l_{(a}n_{b)})$. We use q_{AB} to represent the standard unit sphere metric in angular coordinates $x^A = (\vartheta, \varphi)$ and set $q^{AB} = q^{(A}\bar{q}^{B)}$, where $q^{AB}q_{BC} = \delta^A_C$, with $q^A = (1, i/\sin \vartheta)$. We use q^A to define the $\eth$ operator with the convention $\eth f = q^A \partial_A f$, for a spin-weight 0 function f. Complex conjugation is denoted with a "bar," e.g. $\Re(f) = (f + \bar{f})/2$. The conventions of the present paper result in a different form of the perturbation equations from that originally given by Teukolsky.

II. THE PERTURBATION EQUATIONS

A. The background Schwarzschild metric in outgoing horizon coordinates

The Schwarzschild metric in standard coordinates is

$$ds^2 = -\left(1 - \frac{2M}{r}\right)dt^2 + dr^2\left(1 - \frac{2M}{r}\right)^{-1} + r^2 q_{AB}dx^A dx^B. \tag{2.1}$$

In outgoing Eddington-Finkelstein coordinates, where $\tilde{u} = t - r^*$ is a null coordinate and $r^* = r + 2M\log(r/2M - 1)$, the Schwarzschild metric takes the Bondi form

$$ds^2 = -\left(1 - \frac{2M}{r}\right)d\tilde{u}^2 - 2d\tilde{u}dr + r^2 q_{AB}dx^A dx^B. \tag{2.2}$$

These coordinates specialize to spherical symmetry the general procedure for constructing a Bondi null coordinate system [24]. They patch two quadrants of the Kruskal manifold: the exterior spacetime quadrant and the quadrant following the initial singularity.

For the anticipated comparison with a fully nonlinear description of a white hole, it is useful to introduce another null coordinate system based upon the affine parameter $u = -Me^{-\tilde{u}/4M}$ along the ingoing null hypersurface $r = 2M$ that forms the white hole horizon. We set $u = 0$ at the intersection of the black hole and white hole horizons, i.e. at the $r = 2M$ bifurcation sphere (corresponding to $\tilde{u} = +\infty$ in Eddington-Finkelstein coordinates). The metric then becomes

$$ds^2 = -\left(1 - \frac{2M}{r}\right)\frac{16M^2}{u^2}du^2 + \frac{8M}{u}dudr + r^2 q_{AB}dx^A dx^B.$$

$$(2.3)$$

In addition, we introduce an affine parameter λ along the outgoing null geodesics in the r direction, with the affine freedom fixed by requiring that $\lambda = 0$ when $r = 2M$ and that $g^{ab}(\partial_a u)\partial_b \lambda = -1$. This implies

$$\lambda = -\frac{4M(r - 2M)}{u}.$$

In these (u,λ) coordinates, the metric takes the form

$$ds^2 = -Wdu^2 - 2dud\lambda + r^2 q_{AB}dx^A dx^B, \qquad (2.4)$$

where

$$r = 2M - \frac{\lambda u}{4M} \qquad (2.5)$$

and

$$W = \frac{2\lambda^2}{\lambda u - 8M^2}. \qquad (2.6)$$

These coordinates specialize to spherical symmetry the general procedure for constructing a Sachs null coordinate system designed for the double-null initial value problem [7]. For this reason, they are especially useful for the study of horizons in the nonlinear regime. They are also useful in the perturbative regime because they cover the entire Kruskal manifold $r > 0$ with remarkably simple analytic behavior, as first discovered by Israel [25]. Since $g^{\lambda\lambda} = W = -\lambda^2/(2Mr)$ the hypersurfaces $\lambda = $ const are everywhere spacelike (so that the u-direction is spacelike) except on the white hole horizon where $\lambda = 0$ and the u-direction is null. The surfaces $u = $ const are everywhere null. The spacelike surfaces $\lambda = $ const > 0 ($\lambda = $ const < 0 can be used as partial Cauchy hypersurfaces to cover the two quadrants above (below) $\lambda = 0$ in the Kruskal manifold.

B. The Teukolsky equations

By aligning a complex null tetrad, $(l^\mu, n^\mu, m^\mu, \bar{m}^\mu)$ with the degenerate principal null directions of a Petrov type D background spacetime, Teukolsky [2] was able to express the vacuum perturbation equations for the Weyl curvature scalars $\psi_0 = C_{abcd}l^a m^b l^c m^d$ (of spin-weight $s = 2$) and $\psi_4 = C_{abcd}n^a \bar{m}^b n^c \bar{m}^d$ (of spin-weight $s = -2$) of the Newman-Penrose (NP) formalism [26] as the simple wave equations

$$[(D + 3\epsilon - \bar{\epsilon} + 4\rho + \bar{\rho})(\Delta + 4\gamma - \mu) - (\delta - \bar{\pi} + \bar{\alpha} + 3\beta + 4\tau)$$

$$\times(\bar{\delta} - \pi + 4\alpha) - 3\psi_2]\psi_0 = 0, \qquad (2.7)$$

$$[(\Delta - 3\gamma + \bar{\gamma} - 4\mu - \bar{\mu})(D - 4\epsilon + \rho) - (\bar{\delta} + \bar{\tau} - \bar{\beta} - 3\alpha - 4\pi)$$

$$\times(\delta + \tau - 4\beta) - 3\psi_2]\psi_4 = 0. \qquad (2.8)$$

Here the spin coefficients $\alpha = (l_{a;b}n^a \bar{m}^b - m_{a;b}\bar{m}^a \bar{m}^b)/2$, $\beta = (l_{a;b}n^a m^b - m_{a;b}\bar{m}^a m^b)/2$, $\gamma = (l_{a;b}n^a n^b - m_{a;b}\bar{m}^a n^b)/2$, $\epsilon = (l_{a;b}n^a l^b - m_{a;b}\bar{m}^a l^b)/2$, $\tau = l_{a;b}m^a n^b$, $\pi = -n_{a;b}\bar{m}^a l^b$, $\rho = l_{a;b}m^a \bar{m}^b$ and $\mu = -n_{a;b}\bar{m}^a m^b$ are computed using the background geometry and the directional derivatives are $D = l^a \partial_a$, $\Delta = n^a \partial_a$, $\delta = m^a \partial_a$ and $\bar{\delta} = \bar{m}^a \partial_a$. The Weyl scalars ψ_0 or ψ_4 are first order quantities in perturbation theory while $\psi_2 = C_{abcd}l^a m^b \bar{m}^c n^d = -M/r^3$ is a zeroth order curvature quantity.

This formulation has several advantageous features: (i) It is a completely first order gauge invariant description (i.e., the perturbative Weyl scalars ψ_0 or ψ_4 are invariant not only under infinitesimal coordinate transformations but also under null rotations of the tetrad); (ii) It does not rely on any frequency or multipole decomposition (i.e., the above equations can be directly integrated in the time domain); (iii) The Weyl scalars are objects defined in the full nonlinear theory, where ψ_0 can be prescribed as constraint-free data on an outgoing null hypersurface and ψ_4 as constraint-free data on an ingoing null hypersurface.

Since Eqs. (2.7),(2.8) are expressed in a covariant form, it is straightforward to write them explicitly in any background coordinate system. Specializing thus to the Schwarzschild background metric in the Israel coordinates introduced in Eq. (2.4), we choose a null tetrad

$$l^a = -\nabla^a u = \left(\frac{\partial}{\partial\lambda}\right)^a = [0,1,0,0],$$

$$n^a = \left(\frac{\partial}{\partial u}\right)^a - \frac{W}{2}\left(\frac{\partial}{\partial\lambda}\right)^a = \left[1, \frac{\lambda^2}{4Mr}, 0, 0\right],$$

$$m^a = \frac{1}{\sqrt{2}r}q^a,$$

$$\bar{m}^a = \frac{1}{\sqrt{2}r}\bar{q}^a, \qquad (2.9)$$

where

$$q^a = \left(\frac{\partial}{\partial\vartheta}\right)^a + \frac{i}{\sin\vartheta}\left(\frac{\partial}{\partial\varphi}\right)^a = [0,0,q^A]. \qquad (2.10)$$

Correspondingly, the only non-vanishing background NP quantities are

$$\alpha = -\beta = \frac{\cot(\vartheta)}{2\sqrt{2}r}, \qquad \gamma = \frac{(r+2M)\lambda}{8Mr^2},$$

$$\mu = \frac{\lambda}{2r^2}, \qquad \rho = -\frac{u}{4Mr},$$

$$D = \frac{\partial}{\partial\lambda}, \qquad \Delta = \frac{\partial}{\partial u} + \frac{\lambda^2}{4Mr}\frac{\partial}{\partial\lambda},$$

$$\delta = \frac{1}{\sqrt{2}\,r}\left(\frac{\partial}{\partial\vartheta} + \frac{i}{\sin\vartheta}\frac{\partial}{\partial\varphi}\right),$$

$$\bar{\delta} = \frac{1}{\sqrt{2}\,r}\left(\frac{\partial}{\partial\vartheta} - \frac{i}{\sin\vartheta}\frac{\partial}{\partial\varphi}\right). \qquad (2.11)$$

Substitution of the above NP quantities into Eqs. (2.7),(2.8) reduces the Teukolsky equations to

$$\left(L_0 + \frac{L^2}{2r^2}\right)\psi_0 = 0 \quad \text{and} \quad \left(L_4 + \frac{L^2}{2r^2}\right)\psi_4 = 0, \qquad (2.12)$$

where

$$L_0 = \frac{1}{4Mr}\lambda^2\partial_\lambda^2 + \partial_u\partial_\lambda - \frac{5}{4Mr}u\partial_u$$

$$- \frac{1}{2Mr^2}\lambda(3M - 4r)\partial_\lambda + \frac{5}{2rM},$$

$$L_4 = \frac{1}{4Mr}\lambda^2\partial_\lambda^2 + \partial_u\partial_\lambda - \frac{1}{4Mr}u\partial_u - \frac{7}{2r^2}\lambda\partial_\lambda$$

$$- \frac{r^2 - 16M^2 + 4Mr}{2Mr^3} \qquad (2.13)$$

and $L^2 = -\bar{\delta}\delta$ is the angular momentum squared operator. In order to treat the radiation near $\mathcal{I}^+$ it is also advantageous to consider a boosted tetrad $(\tilde{l}^a, \tilde{n}^a, m^a, \bar{m}^a)$, with $\tilde{l}^a = -\nabla\tilde{u}$ and $\tilde{n}^a$ satisfying $\tilde{l}^a\tilde{n}_a = -1$. We accordingly define boosted Weyl scalars $\tilde{\psi}_0 = C_{abcd}\tilde{l}^a m^b \tilde{l}^c m^d$ and $\tilde{\psi}_4 = C_{abcd}\tilde{n}^a\bar{m}^b\tilde{n}^c\bar{m}^d$. This boosted tetrad is adapted to the affine time $\tilde{u}$ at $\mathcal{I}^+$ rather than the affine time u at the horizon.

C. Spin-weight-zero versions of the Teukolsky equations

It is useful to convert Eqs. (2.12),(2.13) into spin-weight-zero equations. Considering the commutation relation $(\bar{\delta}\delta - \delta\bar{\delta})\eta = 2s\,\eta$ for a spin-weight s function η, and setting $\psi_0 = \delta^2\Phi_0$ so that $\bar{\delta}\delta\psi_0 = \delta^2(6 + \bar{\delta}\delta)\Phi_0$, the Teukolsky equation for ψ_0 becomes, after factoring out an overall δ^2,

$$\left[\frac{1}{4Mr}\lambda^2\partial_\lambda^2 + \partial_u\partial_\lambda - \frac{5}{4Mr}u\partial_u - \frac{1}{2Mr^2}\lambda(3M - 4r)\partial_\lambda\right.$$

$$\left. + \frac{5}{2rM} - \frac{(6 + \bar{\delta}\delta)}{2r^2}\right]\Phi_0 = 0. \qquad (2.14)$$

Similarly, setting $\psi_4 = \bar{\delta}^2\Phi_4$ so that $\bar{\delta}\delta\psi_4 = \bar{\delta}^2(2 + \bar{\delta}\delta)\Phi_4$ and after factoring out an overall $\bar{\delta}^2$, the Teukolsky equation for Φ_4 takes the spin-weight-zero form

$$\left[\frac{1}{4Mr}\lambda^2\partial_\lambda^2 + \partial_u\partial_\lambda - \frac{1}{4Mr}u\partial_u - \frac{7}{2r^2}\lambda\partial_\lambda\right.$$

$$\left. - \frac{r^2 - 16M^2 + 4Mr}{2Mr^3} - \frac{(2 + \bar{\delta}\delta)}{2\,r^2}\right]\Phi_4 = 0. \qquad (2.15)$$

These equations can be re-expressed in terms of the Laplacian

$$D^2 = -\frac{2\lambda(16M^2 - u\lambda)}{(8M^2 - u\lambda)^2}\partial_\lambda - 2\partial_u\partial_\lambda - \frac{2\lambda^2}{8M^2 - u\lambda}\partial_\lambda^2, \qquad (2.16)$$

defined by the metric $d\bar{s}^2 = -Wdu^2 - 2dud\lambda$ induced by the Schwarzschild metric on the 2-dimensional (u, λ) subspace. Discussion of the asymptotic behavior of the Weyl tensor is most convenient in terms of the variables $F_0 = r^5\Phi_0$ and $F_4 = r\Phi_4$. The spin-weight-zero Eqs. (2.14) and (2.15) then reduce to

$$(D^2 + T_0)F_0 = 0 \qquad (2.17)$$

$$(D^2 + T_4)F_4 = 0, \qquad (2.18)$$

where

$$T_0 = -\frac{(6M + r)\lambda}{Mr^2}\partial_\lambda - \frac{30M}{r^3} + \frac{(6 + \bar{\delta}\delta)}{r^2}$$

and

$$T_4 = \frac{(6M + r)\lambda}{Mr^2}\partial_\lambda - \frac{6M}{r^3} + \frac{(2 + \bar{\delta}\delta)}{r^2}$$

do not contain ∂_u terms.

Asymptotic flatness requires that F_0 and F_4 have finite limits at $\mathcal{I}^+$. This is consistent with the asymptotic forms of Eqs. (2.17) and (2.18), which asymptote to one-dimensional wave equations for solutions whose radial derivative falls off uniformly as $O(1/r^2)$. The limit of F_4 determines the outgoing gravitational radiation wave form and the limit of F_0 is related to the retarded quadrupole moment of the system. More precisely, $\lim r\tilde{\psi}_4^0 = \partial_{\tilde{u}}\bar{N}$, where N is the standard definition of the Bondi news function.

In the limit $\lambda \to \infty$,

$$\frac{(6M + r)\lambda}{Mr^2} \to -\frac{4}{u},$$

so that the appearance of this term in T_0 and T_4 can cause inaccuracy in the numerical solution of Eqs. (2.17) and (2.18) at late Bondi times on $\mathcal{I}^+$ (as $-u \to 0$). In particular, the late time behavior of the radiation wave form, can be more accurately computed by an evolution algorithm for the Weyl component $\tilde{\psi}_4$. Setting $\tilde{\psi}_0 = \delta^2\tilde{\Phi}_0$ and $\tilde{\psi}_4 = \bar{\delta}^2\tilde{\Phi}_4$, the fields $\tilde{F}_0 = r^5\tilde{\Phi}_0$ and $\tilde{F}_4 = r\tilde{\Phi}_4$ satisfy

$$(D^2 + S_0)\widetilde{F}_0 = 0, \qquad (2.19)$$

$$(D^2 + S_4)\widetilde{F}_4 = 0, \qquad (2.20)$$

where

$$S_0 = \frac{16M(r-3M)}{ur^2}\partial_\lambda - \frac{30M}{r^3} + \frac{(6+\eth\bar\eth)}{r^2}$$

$$= -\frac{4(r-3M)}{r^2}\partial_r - \frac{30M}{r^3} + \frac{(6+\bar\eth\eth)}{r^2}$$

and

$$S_4 = -\frac{16M(r-3M)}{ur^2}\partial_\lambda - \frac{6M}{r^3} + \frac{(2+\bar\eth\eth)}{r^2}$$

$$= \frac{4(r-3M)}{r^2}\partial_r - \frac{6M}{r^3} + \frac{(2+\bar\eth\eth)}{r^2}.$$

In these variables, the deviation of the Teukolsky equations (2.19) and (2.20) from a one-dimensional wave equation is independent of time at a fixed r. These equations are well behaved at $\mathcal{I}^+$, i.e., after a compactified coordinate such as $x = 1/r$ is introduced. Because $\widetilde{F}_4 = (u/4M)^2 F_4$, where F_4 must be regular throughout the Kruskal manifold (since it is constructed with a regular basis), it follows that $\widetilde{F}_4 \to 0$ as the black hole horizon is approached. This facilitates an accurate long term evolution of the wave form using Eq. (2.20).

Note also, however, that $\widetilde{F}_0 = (4M/u)^2 F_0$ so that $\widetilde{F}_0$ is singular on the black hole horizon and thus a poor choice of variable for long term evolution. The opposite signs of the coefficients of ∂_r in S_0 and S_4 are responsible for this behavior, as can be seen by ignoring the remaining potential terms and freezing the coefficient of ∂_r at $r = 2M$, so that Eqs. (2.19) and (2.20) reduce to

$$\left(2\partial_{\widetilde{u}} - \partial_r - \frac{1}{M}\right)\partial_r\widetilde{F}_0 = 0, \qquad (2.21)$$

$$\left(2\partial_{\widetilde{u}} - \partial_r + \frac{1}{M}\right)\partial_r\widetilde{F}_4 = 0, \qquad (2.22)$$

in terms of retarded Bondi coordinates. In this approximation, both of these equations admit purely outgoing waves $\widetilde{F}(\widetilde{u})$. However, an ingoing $\widetilde{F}_0$ wave has the exponentially singular behavior

$$\widetilde{F}_0 = f(\widetilde{u} + 2r)e^{(\widetilde{u} - \widetilde{u}_0)/2M}$$

as an initial pulse $f(\widetilde{u}_0 + 2r)$ approaches the black hole horizon as $\widetilde{u} \to \infty$. In contrast, an ingoing $\widetilde{F}_4$ wave decays exponentially on approach to the black hole.

D. Time reflection properties of the Teukolsky equation

The different forms of Eqs. (2.14) and (2.15), or Eqs. (2.19) and (2.20), make it clear that the Teukolsky equation for the Weyl component ψ_0 in the outgoing null direction l^a and the Teukolsky equation for the Weyl component ψ_4 in the ingoing null direction n^a are not related in a way which makes manifest the time reflection symmetry $\mathcal{T}$ of the background Schwarzschild geometry, defined by $\mathcal{T}(t,r,\theta,\phi) = (-t,r,\theta,\phi)$ in Schwarzschild coordinates or by $\mathcal{T}(\widetilde{u},r,\theta,\phi) = (-\widetilde{v},r,\theta,\phi)$ in terms of Bondi retarded and advanced times $\widetilde{u} = t - r^*$ and $\widetilde{v} = t + r^*$. The time reflection symmetry could be incorporated explicitly by introducing null tetrad vectors $L^a = \alpha l^a$ and $N^a = (1/\alpha)n^a$ satisfying $\mathcal{T}L^a = -N^a$. However, the explicit form of the required boost,

$$\alpha = -\frac{2M}{u}\sqrt{\frac{2(r-2M)}{r}} = -\frac{2M}{u}\sqrt{\frac{-2\lambda u}{8M^2 - \lambda u}}, \qquad (2.23)$$

makes it clear that such a time symmetric formulation would introduce singular behavior at both the black and white hole horizons.

However, this time symmetric tetrad is useful for formulating the time reflection symmetry of solutions of the Teukolsky equations using other tetrads. Let $\Psi_4 = C_{abcd}N^a m^b N^c m^d = \Psi(\widetilde{u},r,\theta,\phi)$ be a perturbative solution for Ψ_4. Then the time reflection symmetry implies that $\Psi_0 = C_{abcd}L^a\bar{m}^b L^c\bar{m}^d = \bar\Psi(-\widetilde{v},r,\theta,\phi)$ is a perturbative solution for Ψ_0. This correspondence maps a retarded solution (no incoming radiation) for Ψ_4 into an advanced solution (no outgoing radiation) for Ψ_0. In terms of the l^a and n^a Weyl components, the solution $\psi_4 = \psi(\widetilde{u},r,\theta,\phi)$ corresponds under time reflection to the solution

$$\psi_0 = \frac{r^2}{256M^2}e^{r/m}\bar\psi(-\widetilde{v},r,\theta,\phi). \qquad (2.24)$$

III. NULL DATA FOR A SCHWARZSCHILD PERTURBATION

The Weyl component ψ_0 can be posed as constraint-free gravitational data on an outgoing null hypersurface. Similarly, ψ_4 constitutes constraint-free gravitational data on an ingoing null hypersurface. These *nonlinear* results extend to linearized theory but care must be exercised in applying them to the Teukolsky equations.

In the Cauchy formulation, the Teukolsky equation for ψ_4 is normally chosen in order to investigate the outgoing radiation introduced by a perturbation. However, the Hamiltonian and momentum constraints prevent the free specification of ψ_4 (or ψ_0) on a Cauchy hypersurface. Consistent Cauchy data for ψ_4 must be provided indirectly by a 3-metric and extrinsic curvature that solve the constraints. In the Cauchy approach to the close approximation, this has been provided by (a limit of) Misner's time symmetric wormhole data [27]. In the double-null formulation of the characteristic initial

value problem, data are given on a pair of intersecting null hypersurfaces, one outgoing and one ingoing. Null data for the Teukolsky equation for ψ_4 can be freely posed on the ingoing null hypersurface but data for ψ_4 on the outgoing null hypersurface has to obtained indirectly. This can be done, as in the Cauchy problem, by first considering consistent metric data in double null coordinate, from which the Weyl data for ψ_4 can be constructed on both hypersurfaces. This is the method we use here to generate two examples of double-null data for the Teukolsky equation: Robinson-Trautman perturbations and close approximation data.

A. Robinson-Trautman perturbations

The Robinson-Trautman space-times [28] describe an algebraically special but distorted and radiating black hole. They provide an important testbed for the computation of a general perturbative solution by numerical evolution. In the case of outgoing radiation from a black hole of mass M, the metric can be put in the Bondi form [29]

$$ds^2 = -\left(\mathcal{K} - \frac{2M}{r\mathcal{W}}\right)d\tilde{u}^2 - 2\mathcal{W}d\tilde{u}dr$$
$$-2r\mathcal{W}_{,A}d\tilde{u}dx^A + r^2 q_{AB}dx^A dx^B, \quad (3.1)$$

where $\mathcal{K} = \mathcal{W}^2[1 - L^2(\log\mathcal{W})]$, L^2 is the angular momentum operator and $\mathcal{W}(\tilde{u}, x^A)$ satisfies the nonlinear equation

$$12M\partial_{\tilde{u}}(\log\mathcal{W}) = \mathcal{W}^2 L^2 \mathcal{K}. \quad (3.2)$$

The outgoing Eddington-Finkelstein form of the Schwarzschild metric Eq. (2.2) results from setting $\mathcal{W} = 1$. More generally, smooth initial data $\mathcal{W}(\tilde{u}_0, x^A)$ evolve smoothly to form a Schwarzschild black hole horizon. The linearized solutions to the Robinson-Trautman equation (3.2) are obtained by setting $\mathcal{W} = 1 + \phi$ and dropping nonlinear terms in ϕ:

$$12M\partial_{\tilde{u}}\phi = L^2(2 - L^2)\phi. \quad (3.3)$$

For a spherical harmonic perturbation $\phi = A(\tilde{u})Y_{lm}$ this leads to the exponential decay $A = A_0 e^{-\tilde{u}\, l(l+1)(l^2+l-2)/12M}$.

The corresponding Weyl tensor components for the perturbation are $\psi_0 = 0$, in agreement with the role of l^a as an algebraically degenerate principal null direction, and

$$\psi_4 = \frac{2M A_0 [l(l+1) - 2][-6M + l(l+1)r]}{3 r^2 M^2}(-u/M)^{-2+l(l+1)[l(l+1)-2]/3}\bar{\eth}^2 Y_{lm}, \quad (3.4)$$

in terms of the affine horizon parameter u. The perturbation vanishes on the black hole horizon $\mathcal{H}^+$ and is singular at $\mathcal{I}^-$. This supplies the data on $\mathcal{H}^-$ and an outgoing null hypersurface $u = u_-$ for the evolution of ψ_4 forward in retarded time.

For the corresponding time reversed solution, $\psi_4 = 0$. By applying to the Robinson-Trautman perturbations a procedure for mapping an outgoing solution of Einstein's equations into an ingoing version [30], we find the solutions

$$ds^2 = -\left(\mathcal{L} - \frac{2M}{r\mathcal{V}}\right)d\tilde{v}^2 + 2\mathcal{V}d\tilde{v}dr + 2r\mathcal{V}_{,A}d\tilde{v}dx^A + r^2 q_{AB}dx^A dx^B, \quad (3.5)$$

where $\tilde{v}$ is the advanced Bondi time coordinate, $\mathcal{L} = \mathcal{V}^2[1 - L^2(\log\mathcal{V})]$ and

$$12M\partial_{\tilde{v}}(\log\mathcal{V}) = -\mathcal{V}^2 L^2 \mathcal{L}. \quad (3.6)$$

The linearized solutions obtained by setting $\mathcal{V} = 1 + \phi$ satisfy

$$12M\partial_{\tilde{v}}\phi = -L^2(2 - L^2)\phi. \quad (3.7)$$

For a spherical harmonic perturbation $\phi = B(\tilde{v})Y_{lm}$, this leads to the exponential growth $B = B_0 e^{\tilde{v}\, l(l+1)(l^2+l-2)/12M}$. The corresponding perturbative Weyl tensor component is

$$\psi_0 = \frac{B_0 e^{r/M}[l(l+1) - 2][-6M + l(l+1)r](v/M)^{-2+l(l+1)[l(l+1)-2]/3}}{384 M^3}\eth^2 Y_{lm}, \quad (3.8)$$

in terms of $v = Me^{\tilde{v}/4M}$ (the affine parameter along the black hole horizon). This perturbation vanishes on the white hole horizon and is singular at $\mathcal{I}^+$. Nevertheless, it can be used to check a (forward in retarded time) evolution algorithm, beginning at a retarded time u_-, by pasting asymptotically flat initial null data outside some radius to interior Robinson-Trautman data.

B. Close limit initial data

The coordinates introduced by Sachs to formulate the double-null characteristic initial value problem [7] are especially useful when one of the null hypersurfaces is a white hole horizon $\mathcal{H}^-$. Sachs' coordinate system consists of (i) an affine null coordinate u along the generators of $\mathcal{H}^-$, which foliates $\mathcal{H}^-$ into cross-sections and labels the corresponding outgoing null hypersurfaces emanating from the foliation; (ii) angular coordinates x^A which are constant both along the generators of $\mathcal{H}^-$ and along the outgoing rays and (iii) an affine parameter λ along the outgoing rays normalized by $\nabla^\alpha u \nabla_\alpha \lambda = -1$, with $\lambda = 0$ on $\mathcal{H}^-$. In the resulting $x^\alpha = (u, \lambda, x^A)$ coordinates, the metric takes the form

$$ds^2 = -(W - g_{AB}W^A W^B)du^2 - 2dud\lambda$$
$$- 2g_{AB}W^B du dx^A + g_{AB}dx^A dx^B. \qquad (3.9)$$

In addition, it is useful to set $g_{AB} = r^2 h_{AB}$, where $\det(h_{AB}) = \det(q_{AB})$, where q_{AB} is the unit sphere metric.

The requirement that $\mathcal{H}^-$ be null implies that $W = 0$ on $\mathcal{H}$ and the gauge freedom on $\mathcal{H}^-$ can be fixed by choosing the shift so that ∂_u is tangent to the generators, implying that $W^A = 0$ on $\mathcal{H}^-$, and by choosing the lapse so that u is an affine parameter, implying that $\partial_\lambda W = 0$ on $\mathcal{H}^-$. In addition to these choices, we fix the affine freedom in u by specifying it on a slice $\mathcal{S}^-$ of $\mathcal{H}^-$, which is located at an early time approximating the asymptotic equilibrium of the white hole at past time infinity I^-. The outgoing null hypersurface $\mathcal{J}^-$ emanating from $\mathcal{S}^-$ then approximates past null infinity $\mathcal{I}^-$. The Schwarzschild metric in Israel coordinates (2.4) is obtained in the spherically symmetric case when $W^A = 0$ and $h_{AB} = q_{AB}$.

The double-null problem for the close limit of a white hole is posed on the ingoing null hypersurface $\mathcal{H}^-$ and the outgoing null hypersurface $\mathcal{J}^-$, which extends to $\mathcal{I}^+$. In order to pose the double-null Teukolsky problem for ψ_4 in the perturbative regime, we generate the data for ψ_4 from metric data for the nonlinear version of the problem. The metric version of the null data consists of the values of the spin-weight-two field $J = q^A q^B h_{AB}/2$ on $\mathcal{H}^-$ and $\mathcal{J}^-$. For a perturbation of a Schwarzschild background, r is given by Eq. (2.5). On the event horizon $\mathcal{H}^-$,

$$\bar{\psi}_4 = \frac{1}{2}J_{,uu} - \frac{1}{2}J_{,u}KK_{,u} + \frac{1}{4}JK_{,u}^2$$

$$+ J_{,u}r^{-1}r_{,u} + Jr^{-1}r_{,uu} + \frac{1}{4}J_{,u}^2\bar{J}$$

where $K = \sqrt{1 + J\bar{J}}$, which reduces in the linear regime to

$$\bar{\psi}_4 \approx \frac{1}{2}J_{,uu}. \qquad (3.10)$$

Off the horizon the expression for $\bar{\psi}_4$ is more complicated and involves W and W^A as well as J and r.

The horizon data for a head-on fission of a white hole, can be obtained from a conformal model based upon an ingoing

null hypersurface emanating from a prolate spheroid embedded in a flat space [4]. Let $(\hat{r}, \theta, \phi)$ be standard spherical coordinates for the inertial time slices $\hat{t} = $ const of Minkowski space. In the close limit, the eccentricity of the spheroid vanishes and the Minkowski null hypersurface reduces to the light cone from a sphere $\hat{t} = 0$, $\hat{r} = a$. The perturbation of its conformal null geometry is described, to linear order in the eccentricity, by

$$J(\hat{t}, \theta) = -\frac{a\sin^2\theta}{\hat{t} - a}, \qquad (3.11)$$

where the relation between $\hat{t}$ and the affine parameter u on the white hole horizon is

$$\frac{d\hat{t}}{du} = \Lambda(\hat{\tau}) = \frac{\hat{\tau}^2(\hat{\tau} - 1)^2}{(3 - 5\hat{\tau} + \hat{\tau}^2)^2}\left(\frac{(5 - \sqrt{13}) - 2\hat{\tau}}{(5 + \sqrt{13}) - 2\hat{\tau}}\right)^{4/\sqrt{13}}, \qquad (3.12)$$

in terms of

$$\hat{\tau} = \frac{\hat{t} - a}{p}. \qquad (3.13)$$

Here p and a are positive parameters which adjust the affine freedom in the position of the Minkowski null cone on the white hole horizon. At early times Eq. (3.12) implies $u \sim \hat{t}$ but as the Minkowski null cone pinches off at $\hat{t} = a$ the corresponding affine time on the white hole horizon asymptotes to $u \to \infty$. In terms of the inverted pair-of-pants picture for a white hole fission, the pants legs are mapped to $u = \infty$ so that in the close limit the individual white holes are mapped to I^+ along the white hole horizon in the Kruskal manifold. The details are discussed elsewhere in a treatment of fully nonlinear null data for the general two black hole problem [31,32].

Close limit data for $J(u, \theta)$ on the white hole horizon is determined by integrating Eq. (3.12) and substituting into Eq. (3.11). These equations allow the rescaling $u \to Ku$, $\hat{t} \to K\hat{t}$, $p \to Kp$ and $a \to Ka$ which allow us to set $p = 1$ without any loss of generality. Note, that the rescaling $u \to Ku$ is equivalent to the time translation isometry $\tilde{u} \to \tilde{u} + $ const. In order to eliminate nonessential parameters, we initiate the integration at the bifurcation sphere $u = 0$. Then, up to scale, the close data are determined by $\hat{\tau}_0 = \hat{\tau}|_{u=0} < 0$ or in terms of J by the parameter

$$\eta = -\frac{pJ|_{u=0}}{uJ|_{u=\infty}} = -\frac{1}{\hat{\tau}_0}, \qquad (3.14)$$

which is independent of the overall scale freedom $J \to \lambda J$ that is factored out in the close approximation. The parameter η is a scale invariant parameter describing the physical properties of the close limit. It determines the yield of the white hole fission. In the time reversed scenario of a black hole collision, η would be related to the inelasticity of the

collision. No similar parameter seems to appear in the Cauchy description of the close approximation in terms of time symmetric Misner data [6].

The close limit data on the horizon for ψ_4 used in the simulations presented in Sec. V C are obtained by integrating Eq. (3.12) with a fourth order Runga-Kutta scheme and carrying out the substitutions into Eqs. (3.11) and (3.10). The data on an early outgoing null hypersurface are accurately approximated by setting $\psi_4 = 0$ since Eq. (3.11) implies $\psi_4 = O(u^{-3})$. This approximates the condition on the data that there be no ingoing radiation at $\mathcal{I}^-$.

IV. NUMERICAL ALGORITHM

Before giving the details of the numerical algorithm, we should state the goals we want to achieve. For many purposes, it would seem sufficient to evolve the wave form until one can read off the first few cycles of quasinormal mode oscillation. This is sufficient in practice to compare with a nonlinear evolution, to get the astrophysically relevant part of the wave form, to compare quasinormal mode results with those in the literature, etc. Instead we define as our criterion of quality the ability to evolve stably and accurately well into the domain where the wave form is dominated by a power law, which requires at least a $1000M$ of Bondi time for our typical data. This turns out to be a rather stringent criterion, which rules out a number of numerical approaches which we have tried. In all such approaches, our overall strategy is to compactify the outgoing null direction and bring $\mathcal{I}^+$ into a finite coordinate distance while maintaining regularity of the equations.

We begin the description of our numerical setup with a discussion of the ingoing null geodesics, which forms the basis of our approach to the numerical solution of the Teukolsky equation. Then we briefly describe a few of the algorithms which do not work completely satisfactorily for the Teukolsky equation, and explain why this is so. We believe that this also provides useful experience for nonlinear studies, where, lacking a stationary background geometry, the source of problems may be much less obvious.

Our present results pertain to the Teukolsky equation for ψ_4, where ψ_4 describes the outgoing radiation through its asymptotic $O(1/r)$ behavior at $\mathcal{I}^+$. The incoming radiation at $\mathcal{I}^-$ is described by ψ_0, which has asymptotic $O(1/r^5)$ behavior at $\mathcal{I}^+$. As a result, an accurate treatment of the Teukolsky equation for ψ_0 requires different numerical methods, which will be described in a forthcoming paper.

A. Ingoing null geodesics

Null geodesics are fundamental to the design of the numerical algorithm since they are the characteristics of the Teukolsky equation. In particular, since we handle the angular part of the spin-weight-zero Teukolsky equation by a spherical harmonic decomposition in which $\eth\bar{\eth} = -l(l+1)$, the relevant characteristics are the radial null geodesics. The outgoing null geodesics are automatically built into the characteristic evolution scheme, which is based upon a retarded

time foliation. The remaining issue is how to effectively incorporate the behavior of the ingoing null geodesics into the algorithm.

Consider first the description of the ingoing null geodesics in a compactified version of Israel coordinates (u, x), where $x = \lambda/(M + \lambda)$ so that $\mathcal{I}^+$ is located at $x = 1$. The analytical simplicity of these coordinates is not matched by their numerical convenience. The ingoing null geodesics satisfy

$$\frac{dx}{du} = -(1-x)^2 \frac{W}{2M} = \frac{(1-x)x^2}{8M(1-x) - ux}.$$

Near $\mathcal{I}^+$ where $1 - x = \delta \ll 1$, this reduces to

$$\frac{d\delta}{du} = \frac{\delta}{u}. \tag{4.1}$$

Hence δ, and the separation between neighboring geodesics near $\mathcal{I}^+$, decays linearly with u and exponentially with $\tilde{u}$. Thus evolving for a Bondi time of $\tilde{u} = 1000M$ is impossible as the geodesics would be within $e^{-250}\delta_0$ of each other.

Not only is the x-coordinate numerically unsatisfactory in the way it compactifies $\mathcal{I}^+$, the u-coordinate is also inconvenient in the way it covers the exterior Kruskal quadrant in a finite retarded time. This prevents the long term numerical resolution of the ringdown (with the characteristic time scale of the lowest quasinormal mode) without using an exponentially decaying step size Δu. This is simple to fix by using Bondi time $\tilde{u}$ as the time step coordinate.

The problem with the x-coordinate can be "delayed" by introducing a dynamical grid, in which the gridpoints move along the ingoing null geodesics, a strategy that has been successful in studies of spherical critical collapse [33]. This approach drastically decreases the discretization error and is sufficient to evolve for about $100M$, and read off the quasinormal ringdown frequency and damping time with good accuracy. However, the Δx intervals between neighboring geodesics decrease exponentially and the approach breaks down once the separation between neighboring gridpoints falls below the error of the geodesic integrator (e.g. machine precision) and a "numerical crossing" of the geodesics effectively occurs.

Note that in practice the computation of the null geodesics is related to the problem of inverting the definition of the tortoise coordinate

$$r^* = r + 2M \log\left(\frac{r}{2M} - 1\right)$$

to compute r, which is also required for our production algorithm as discussed in the next section. Both problems are handled numerically by solving the above implicit equation iteratively using Newton's method (in terms of the appropriate coordinates).

B. Numerical algorithm for outgoing radiation

The preceding considerations lead us to the following choice of algorithm for a production level unigrid code with

optimal performance. It is based on a $(\tilde{u}, \rho)$ coordinate system, where ρ is a radial coordinate, which compactifies $\mathcal{I}^+$, defined implicitly by

$$r^* = \rho_0 \tan \rho, \qquad (4.2)$$

with ρ_0 an adjustable parameter and $-\pi/2 \leq \rho \leq \pi/2$. The ρ coordinate allows good resolution at all times near both $\mathcal{I}^+$ and the white hole horizon.

In this coordinate system, we evolve the lth spherical harmonic component of $\tilde{F}_4$ by expressing the second order differential equation (2.20) as the two coupled equations

$$\partial_\rho \tilde{F}_4 = G \qquad (4.3)$$

$$\partial_{\tilde{u}} G = \frac{\cos^2 \rho}{2\rho_0} \partial_\rho G + \left(2 \frac{(r - 3M)}{r^2} - \frac{\sin \rho \cos \rho}{\rho_0} \right) G$$

$$- \frac{\rho_0}{\cos^2 \rho} \frac{(r - 2M)[(l^2 + l - 2)r + 6M]}{2r^4} \tilde{F}_4. \quad (4.4)$$

The background mass M can be scaled out of the above equations by the rescaling $\rho_0 \to M\rho_0$, $\tilde{u} \to M\tilde{u}$ and $r \to Mr$. In this way, simulations can be carried out with $M = 1$ without loss of generality. Note that rescaling $\tilde{u}$ is independent of the rescaling $u \to Ku$ (see Sec. III B) which generates the translation isometry of $\tilde{u}$.

The relatively sensitive features of Eq. (4.4) on a hypersurface of constant $\tilde{u}$ are located in the region near $r = 2M$. This is the main reason why the ρ coordinate is so useful since it concentrates grid points in that region while maintaining a uniform grid spacing. We make the choice $\rho_0 = 40M$, which gives good resolution throughout the evolution, well past the ringdown phase and into the final power law tail. Note that this would not be possible with the simpler approach of writing the Teukolsky equation in (a compactified version of) double null coordinates $(\tilde{u}, \tilde{v})$, which gives excellent results until one reaches the power law tail. At this stage the dynamics is essentially dominated by the ''Schwarzschild potential,'' which is not well resolved in double null coordinates.

Equation (4.3) is solved using a second order accurate integration in ρ. Equation (4.4) is solved using a second order (in time) Runga-Kutta scheme, with the $\partial_\rho G$ term evaluated by means of second order accurate forward differencing in the interior of the grid, and second order accurate central differencing for the point neighboring $\mathcal{I}^+$. (The $\partial_\rho G$ term drops out on both $\mathcal{H}^-$ and $\mathcal{I}^+$, where $\partial_{\tilde{u}}$ is a characteristic direction.)

For a typical choice of initial data the power law tail only sets in after the quasinormal oscillations have decayed by more than 10 orders of magnitude. In order for the final tail not to be lost in machine error it is necessary to evolve the quasinormal phase in quadruple precision.
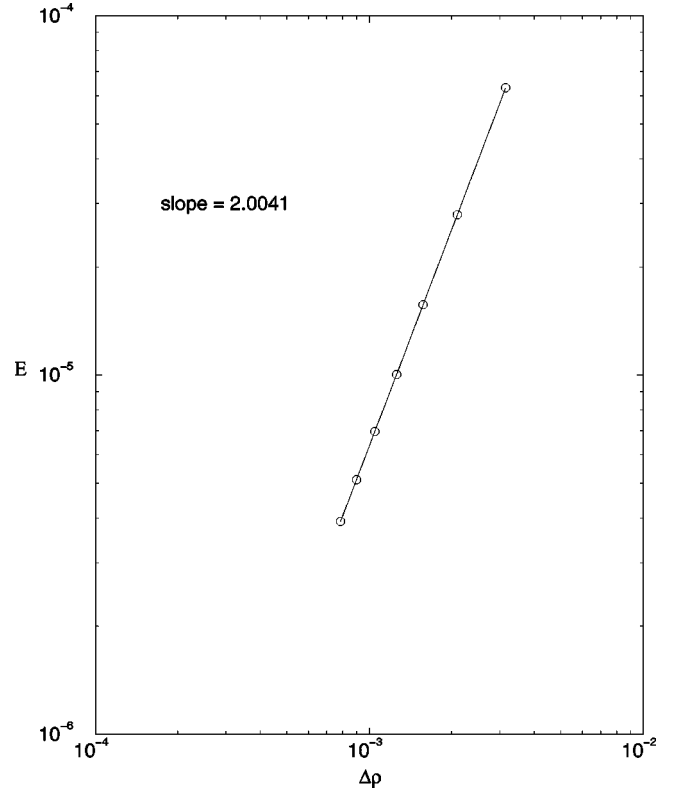

FIG. 1. Robinson-Trautman convergence test: l_∞ error norm E versus gridsize $\Delta\rho$.
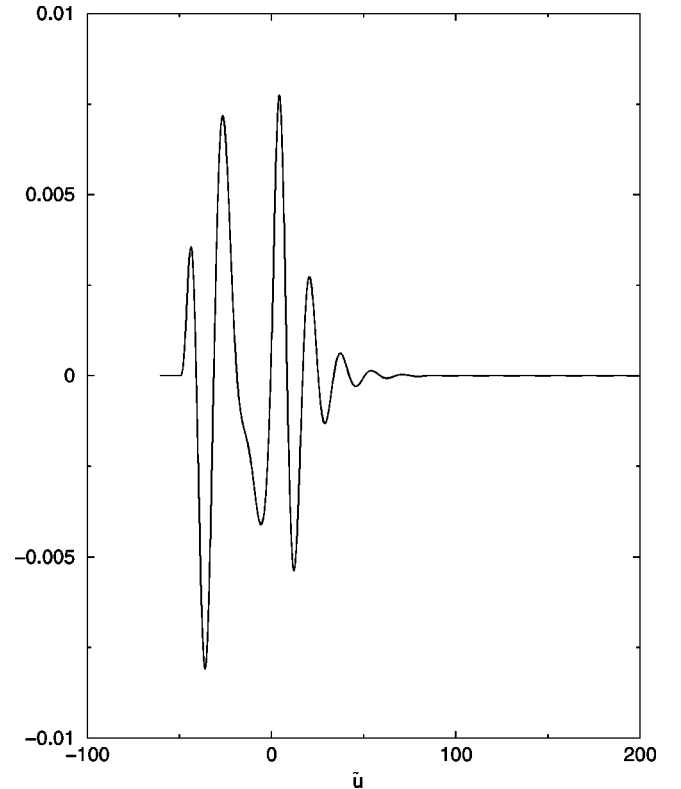

FIG. 2. Wave form $\tilde{F}_4(\tilde{u})$ at $\mathcal{I}^+$ produced by a single pulse emerging from the white hole horizon.
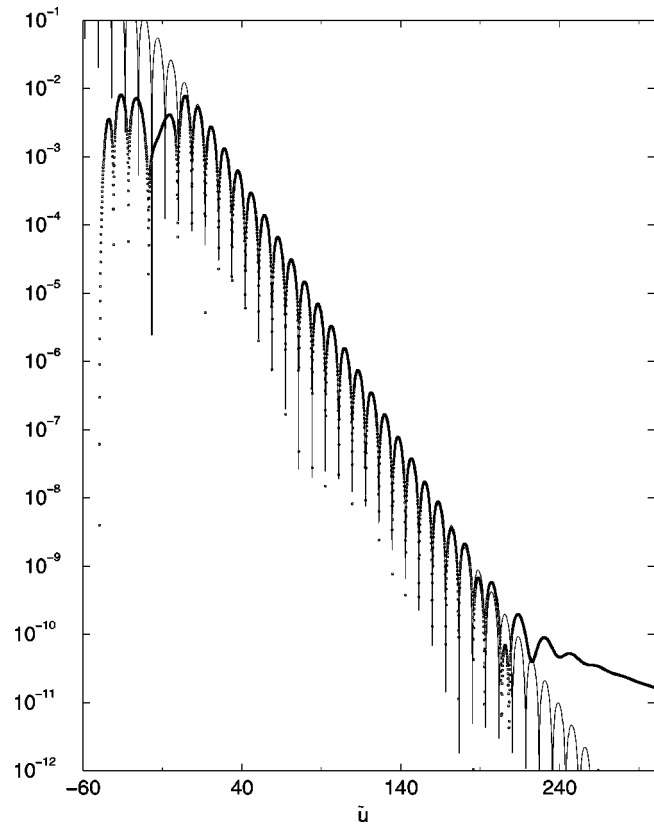
FIG. 3. Log plot of $|\widetilde{F}_4(\widetilde{u})|$ for the wave form in Fig. 2 (darker curve) and a fit to the quasinormal ringdown (lighter curve).
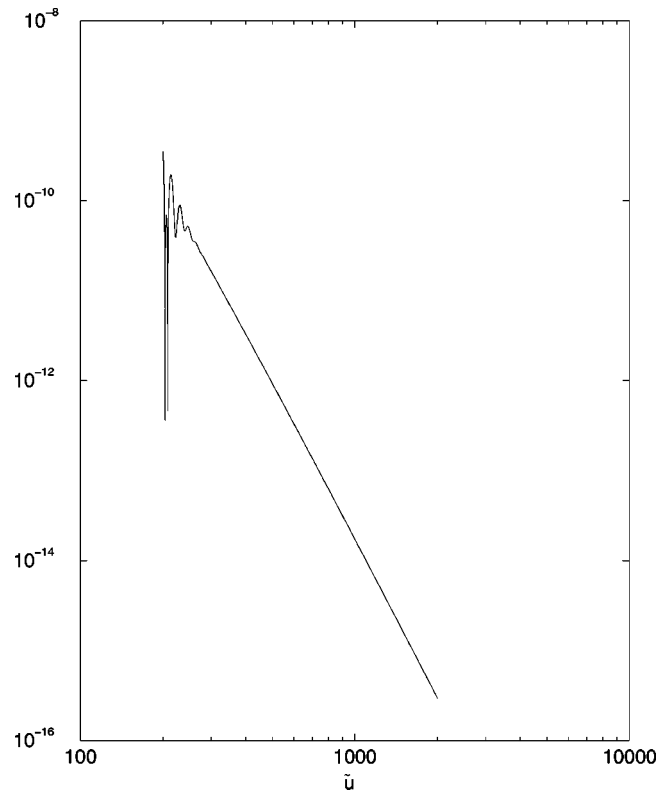

FIG. 5. $\hat{\tau}(u)$ versus u for 4 values of η.

FIG. 4. Log-log plot of the tail of the wave form in Fig. 2.
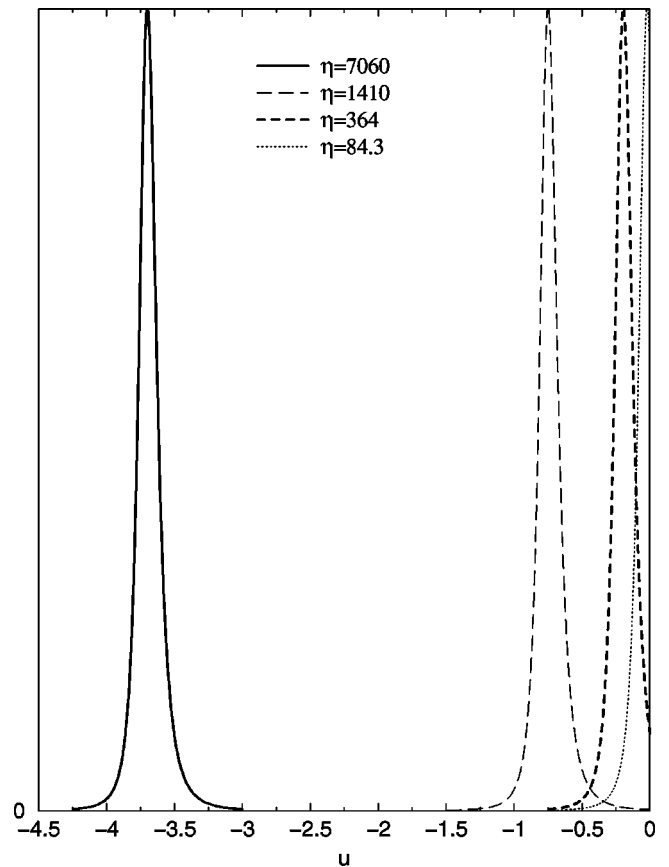

FIG. 6. Close approximation data $F_4(u)$ on $\mathcal{H}^-$ for 4 values of η.
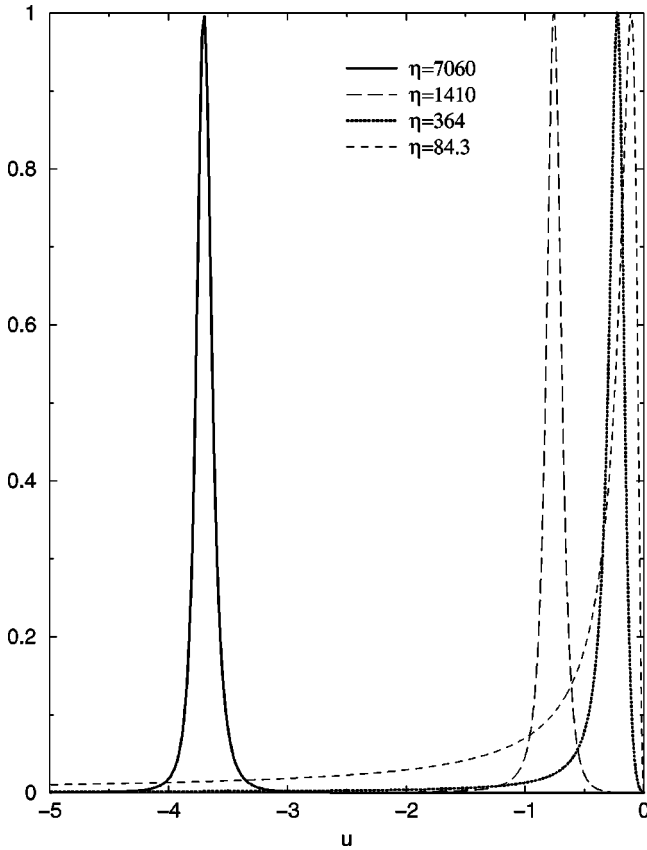
FIG. 7. Close approximation data $\widetilde{F}_4(u)$ on $\mathcal{H}^-$ for $\eta=7060$, 1410, 364 and 84.3, with the amplitudes renormalized by the relative factors of 1, 24.03, 305.9 and 3223, respectively.

FIG. 8. Close approximation data $\widetilde{F}_4(\widetilde{u})$ on $\mathcal{H}^-$ for $\eta=7060$, 1410, 364 and 84.3, with the amplitudes renormalized by the relative factors of 1, 24.03, 305.9 and 3223, respectively.

V. WAVE FORMS

In this section, we present computed wave forms for three types of quadrupole data, with the background mass scaled to $M=1$. The first case, an analytically known Robinson-Trautman perturbation, is used to establish second order convergence of the numerical algorithm. The Robinson-Trautman wave form decays as a pure exponential. The second case, a pulse of compact support emanating from the white hole horizon, serves to monitor the ability of the code to track many cycles of the quasinormal ringdown of a generic radiation tail. The final case is the close limit wave form from a white hole fission.

A. Robinson-Trautman testbed

An $l=2$ Robinson-Trautman perturbation is determined by the spin-weight-0 field

$$\widetilde{F}_4=\frac{r-1}{r}e^{-2\widetilde{u}}. \qquad (5.1)$$

We use this to perform a convergence test of the code by evolving from $\widetilde{u}=0$ to $\widetilde{u}=5$ and then examining the l_∞ norm of the error $E=||\widetilde{F}_{4,NUMERIC}-\widetilde{F}_{4,ANALYTIC}||$ versus grid spacing at $\widetilde{u}=5$, at which time the signal has decreased by a factor of e^{-10}. The convergence plot of the error given in
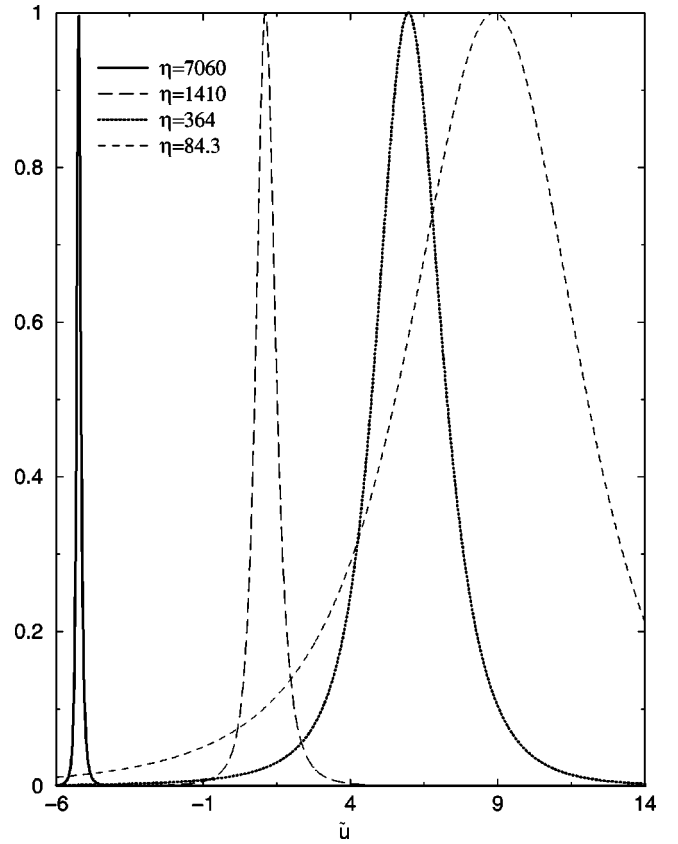
Fig. 1 determines a slope of 2.0041, in excellent agreement with the theoretical second order accuracy of the algorithm.

B. Ringdown from a compact pulse

We simulate the evolution of an $l=2$ quadrupole pulse of compact support emerging from the white hole horizon $\mathcal{H}^-$. The pulse consists of a single peak of the form

$$\widetilde{F}_4(\widetilde{u},x=0)=[(\widetilde{u}-\widetilde{u}_{min})(\widetilde{u}_{max}-\widetilde{u})]^4, \quad \widetilde{u}_{min}<\widetilde{u}<\widetilde{u}_{max}, \qquad (5.2)$$

with $\widetilde{F}_4(\widetilde{u},x=0)=0$ outside this interval. Figure 2 shows the wave form on $\mathcal{I}^+$ obtained by evolving $\widetilde{F}_4$ with initial data $\widetilde{F}_4=0$ on an outgoing hypersurface preceding the pulse. In the simulation used to produce the wave form at $\mathcal{I}^+$, we choose $\widetilde{u}_{min}=-50$ and $\widetilde{u}_{max}=0$ and evolve from $\widetilde{u}=-60M$ to $\widetilde{u}=2000M$. The simulation was performed in two steps. The first step, in the interval from $\widetilde{u}=-60M$ until $\widetilde{u}=250M$, was performed in quadruple precision in order not to lose the final tail in roundoff error. The second step, in the interval from $\widetilde{u}=250M$ until $\widetilde{u}=2000M$, was performed in double precision.

Figure 3 is a logarithmic plot of the absolute value of the wave form versus $\widetilde{u}$ for the same data. It covers the period
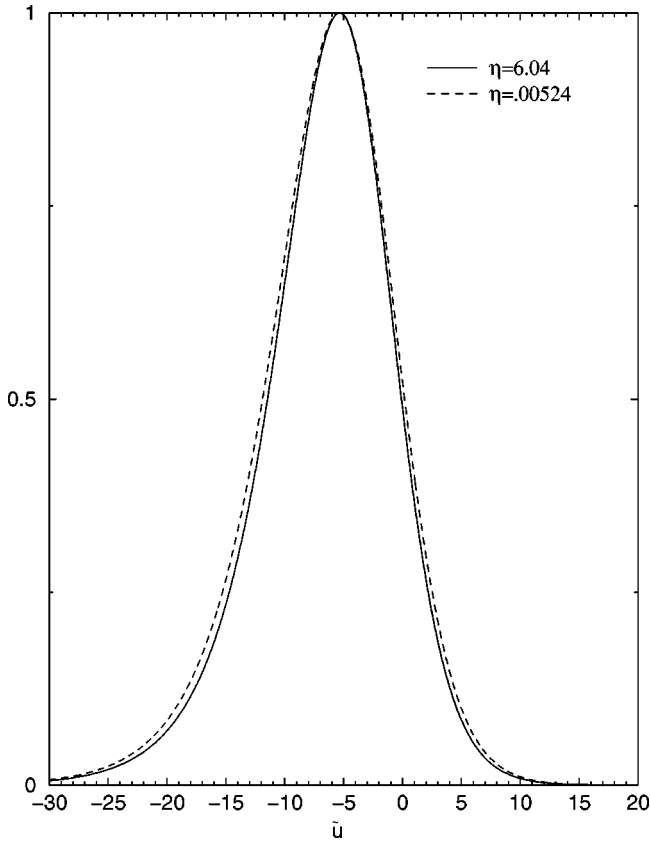
FIG. 9. Close approximation data $\widetilde{F}_4(\widetilde{u})$ on $\mathcal{H}^-$ for $\eta=6.04$ and .00524, with the amplitudes renormalized by the relative factors of 1 and 1220.
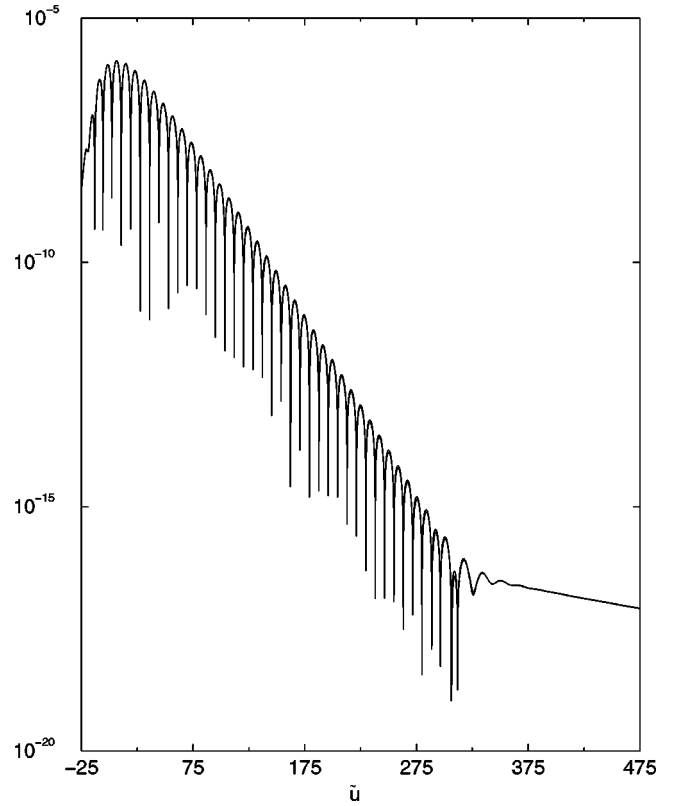

FIG. 10. Convergence of the close approximation wave form at $\mathcal{I}^+$: The overlaid plots of $4\delta y_1(\widetilde{u})$ and $\delta y_2(\widetilde{u})$ are indistinguishable.

from the onset of quasinormal ringdown to the onset of the final tail decay. The logarithmic plot clearly demonstrates the exponential decay and shows a fit to a quasinormal decay. The lowest quasinormal mode for a gravitational perturbation of the Schwarzschild metric has the theoretical form $f \sim \sin(.373672\widetilde{u})\exp(-.0889625\widetilde{u})$ [34]. The fit of the computed wave form to a quasinormal decay is $\widetilde{F}_4 \sim \sin(.373668\widetilde{u})\exp(-.088951\widetilde{u})$, in excellent agreement with the expected theoretical form. The corresponding fit of the close approximation wave form given in Sec. V C yields the quasinormal dependence

$$\widetilde{F}_4 \sim \sin(.3736735\widetilde{u})\exp(-.0889575\widetilde{u}).$$

A conservative comparison of these two calculations indicates a quasinormal dependence $\widetilde{F}_4 \sim \sin(.37367\widetilde{u})\exp(-.08895\widetilde{u})$, with the numerical uncertainty in the last digit.

Figure 4 shows a log-log plot of the late time behavior of the wave form and the final tail. The measured slope of the tail indicates a power law decay, with the power varying from $\widetilde{F}_4 \propto \widetilde{u}^{-5.76}$ near the beginning of the tail to $\widetilde{F}_4 \propto \widetilde{u}^{-5.89}$ near the end.

C. The close approximation wave form

As discussed in Sec. III B, the effective parameter space for the head-on close approximation data can be reduced to the single scale invariant parameter η controlling the fission yield. In the simulations presented here we set the scale dependent parameter $p=1$. Thus, in accord with the discussion in Sec. III B, we identify $\hat{t}-a=\hat{\tau}$ and prescribe the horizon data used in the simulations in the normalized form

$$F_4 = -(\Lambda\partial_{\hat{\tau}})(\Lambda\partial_{\hat{\tau}})\frac{1}{\hat{\tau}}, \tag{5.3}$$

after factoring out the $l=2$ angular dependence.

The time dependence of the close approximation data is quite mild when expressed as a function of $\hat{\tau}$, as in Eq. (5.3). However, the relationship (3.12) can cause the dependence on u to be quite sharp. There is a transition region where the behavior of $\hat{\tau}(u)$ changes from the asymptotic form $d\hat{\tau}/du \rightarrow 1$ as $\hat{\tau} \rightarrow -\infty$ to $d\hat{\tau}/du \rightarrow 0$ as $\hat{\tau} \rightarrow 0$. For large values of the parameter η, this produces sharply pulse shaped data, as described below.

Figure 5 plots $\hat{\tau}$ versus u for $\eta=7060$, 1410, 364, and 84.3. The plots reveal a relatively sharp transition in the slope. This transition region is translated in the negative u-direction as η increases. For sufficiently small η the tran-
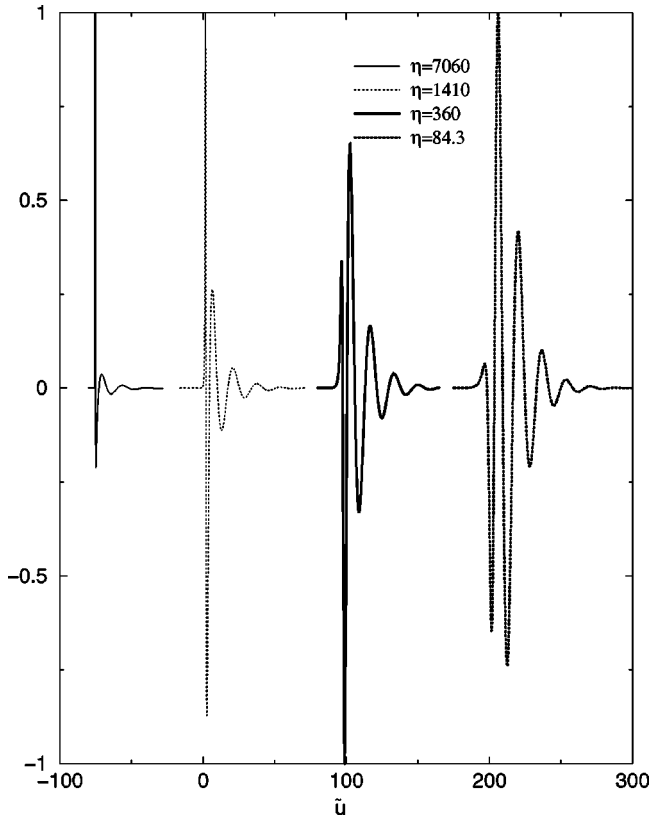
FIG. 11. Close approximation wave forms $\widetilde{F}_4(\widetilde{u})$ on $\mathcal{I}^+$ for $\eta = 7060$, 1400, 368 and 84.3, with the amplitudes renormalized by the relative factors of 1, 37.9, 544 and 11200, respectively.

FIG. 12. Close approximation wave form $\widetilde{F}_4(\widetilde{u})$: Quasinormal ringdown and tail for $\eta = 158$.

sition occurs at $u > 0$, in the region of the white hole horizon which does not affect the exterior spacetime.

The location of the transition region affects the nature of the horizon data. Figure 6 shows $F_4(u)|_{\mathcal{H}^-}$ for the above values of η. The value of η only changes the position of the transition region, not its width. Hence a change in η translates the horizon data $F_4(u)|_{\mathcal{H}^-}$ but does not change its shape.

The horizon data for $\widetilde{F}_4(\widetilde{u})$ has a more complicated dependence on η due to the exponential relationship between u and $\widetilde{u}$ and the extra factor of u^2 introduced by the change in tetrad. This is of physical importance since it is $\widetilde{F}_4(\widetilde{u})$ which is the observed wave form at $\mathcal{I}^+$. The factor of u^2 suppresses pulses centered at smaller $|u|$ compared to those centered at larger $|u|$ and forces the resulting pulse to vanish at $u = 0$. The relation between $\widetilde{u}$ and u varies from an exponentially increasing blueshift at large negative u to an exponentially increasing redshift at $u = 0$. This has the effect of compressing pulses centered at more negative u compared to those centered at less negative u. These effects combine to produce successively broader pulses for successively smaller η. However, once η is sufficiently small, the transition region is located at $u > 0$ and η does not affect the shape of $\widetilde{F}_4(\widetilde{u})|_{\mathcal{H}^-}$, although it affects its overall amplitude. In that case $\hat{\tau} \approx u + \hat{\tau}_0$ for $-\infty < u < 0$, and $F_4|_{\mathcal{H}^-} \propto 1/(u + \hat{\tau}_0)^3$, where $\hat{\tau}_0 = -1/\eta$. As a result, modulo a constant overall
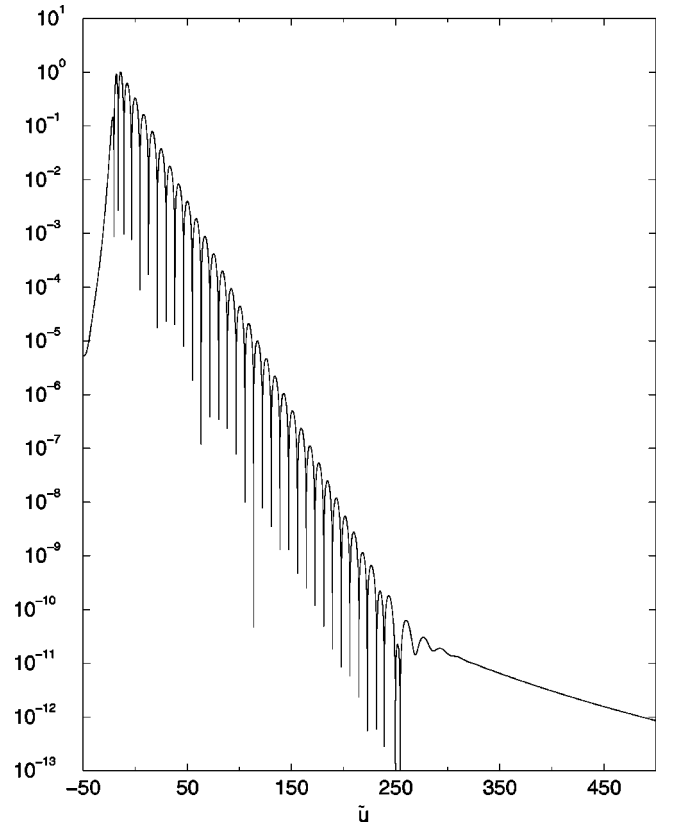
multiplicative factor and a constant shift in $\widetilde{u}$,

$$\widetilde{F}_4(\widetilde{u})|_{\mathcal{H}^-} \propto \frac{\eta e^{-\widetilde{u}/2}}{(e^{-\widetilde{u}/4} + 1)^3}. \tag{5.4}$$

Figures 7 and 8 show $\widetilde{F}_4(u)|_{\mathcal{H}^-}$ and $\widetilde{F}_4(\widetilde{u})|_{\mathcal{H}^-}$, respectively, for $\eta = 7060$, 1410, 364, and 84.3. Figure 9 shows $\widetilde{F}_4|_{\mathcal{H}^-}$ versus $\widetilde{u}$ for small η, with the amplitude and position of the peaks adjusted so that they overlap. Except for the overall amplitude, there is no significant effect on the data even when η is reduced by 3 orders of magnitude. For small values of η, $\widetilde{F}_4(\widetilde{u})|_{\mathcal{H}^-}$ scales linearly with η in accord with Eq. (5.4), whereas for large η it scales quadratically, as evident from the renormalizations in Figs. 7 and 8.

We test the convergence of the wave form at $\mathcal{I}^+$ by evolving this close approximation data with increasingly larger grids containing 1001, 2001, and 4001 points. We define δy_1 to be the difference between the waveforms obtained using 1001 and 2001 points, and δy_2 the difference between using 2001 and 4001 points. (We consider only points common to all three grids.) Second order convergence requires that $\delta y_1 = 4 \delta y_2$. For these grid sizes, Fig. 10 shows that δy_1 and $4 \delta y_2$ overlap confirming that the code is second order convergent throughout the quasinormal ringdown phase.

Figure 11 shows a series of wave forms produced on $\mathcal{I}^+$ obtained by evolving the close approximation data for η
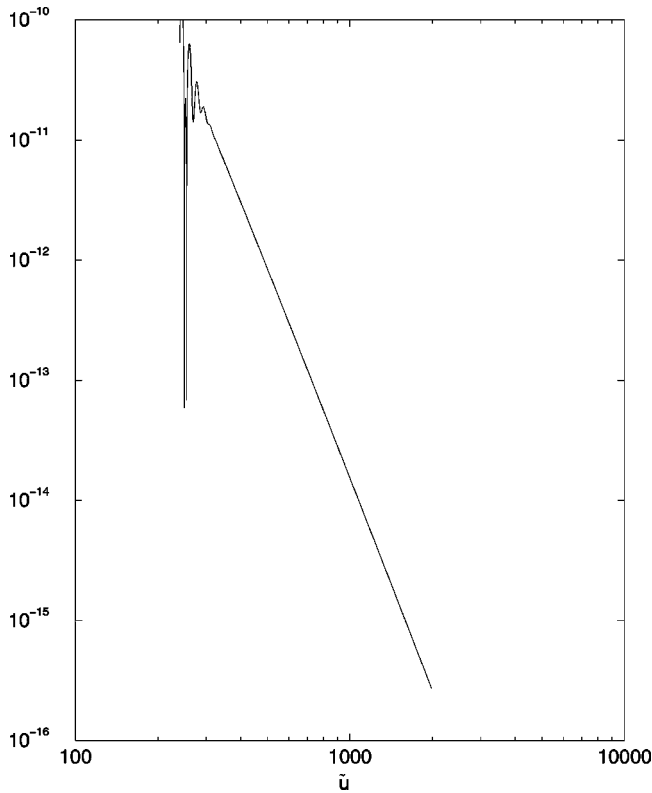
FIG. 13. Close approximation wave form $\widetilde{F}_4(\widetilde{u})$: Late time power law tail for $\eta = 158$.

$=7060$, 1410, 364 and 4.39. The wave forms have been translated with respect to each other and normalized to unit amplitude for purpose of comparison. The plots show the wave forms from the initial time up to (roughly) the onset of quasinormal decay.

Figure 12 shows a log plot of the wave form produced for $\eta = 158$. The fit of the exponentially damped section is

$$\widetilde{F}_4 \propto e^{-.0889575\widetilde{u}}\sin(.3736735\widetilde{u}), \qquad (5.5)$$

which matches the theoretical form for the lowest quasinormal mode to five digits (in the frequency).

Figure 13 shows the late time tail of the wave form. The measured slope of the tail indicates a power law decay of the approximate form $\widetilde{F}_4 \propto \widetilde{u}^{-5.8}$ near the beginning of the tail to $\widetilde{F}_4 \propto \widetilde{u}^{-5.9}$ near the end, very similar to the behavior of the tail for the compact pulse described in Sec. V B. These results suggest a final integer power law tail $\widetilde{F}_4 \propto \widetilde{u}^{-6}$. For an $l = 2$ quadrupole wave, this is the same $\widetilde{u}^{-(2l+2)}$ integer power law originally predicted by Price [35] for the decay of an initially static multipole. A rigorous mathematical treatment of power law tails has not yet been given [36] and it would be particularly interesting to reexamine the theory in the context of our boundary conditions.

VI. DISCUSSION

Our results establish the capability of characteristic evolution of the Teukolsky equation to determine an accurate advanced solution for the head-on collision of black holes in the close approximation. In subsequent work, we will extend these results to determine the physically more appropriate retarded solution. In the fully nonlinear regime, the conformal horizon model for supplying binary black hole data, combined with an existing characteristic evolution code, offers a new way to calculate the merger-ringdown wave form from coalescing black holes. Because this is an unexplored area of binary black hole physics, these perturbative studies of the head-on collision will provide a preliminary physical check on extending the work to the nonlinear and nonaxisymmetric case, where inspiraling black holes can be treated.

[1] Saul A. Teukolsky, Phys. Rev. Lett. **29**, 1114 (1972).

[2] S. A. Teukolsky, Astrophys. J. **185**, 635 (1973).

[3] J. Winicour, Suppl. Prog. Theor. Phys. **136**, 57 (1999).

[4] Luis Lehner, Nigel T. Bishop, Roberto Gómez, Bela Szilágyi, and Jeffrey Winicour, Phys. Rev. D **60**, 044005 (1999).

[5] Nigel T. Bishop, Roberto Gómez, Luis Lehner, Manoj Maharaj, and Jeffrey Winicour, Phys. Rev. D **56**, 6298 (1997).

[6] Richard H. Price and Jorge Pullin, Phys. Rev. Lett. **72**, 3297 (1994).

[7] R. Sachs, J. Math. Phys. **3**, 908 (1962).

[8] S. A. Hayward, Class. Quantum Grav. **10**, 779 (1993).

[9] H. Friedrich, Proc. R. Soc. London **A378**, 401 (1981).

[10] A. H. Rendall, Proc. R. Soc. London **A427**, 221 (1990).

[11] John Baker, Steven Brandt, Manuela Campanelli, Carlos O. Lousto, Edward Seidel, and Ryoji Takahashi, Phys. Rev. D **62**, 127701 (2000).

[12] John Baker, Bernd Brügmann, Manuela Campanelli, and Car-
los O. Lousto, Class. Quantum Grav. **17**, L149 (2000).

[13] R. Gómez *et al.*, Phys. Rev. Lett. **80**, 3915 (1998).

[14] Manuela Campanelli, Gaurav Khanna, Pablo Laguna, Jorge Pullin, and Michael P. Ryan, Class. Quantum Grav. **18**, 1543 (2001).

[15] E. Newman and R. Penrose, J. Math. Phys. **3**, 566 (1962).

[16] J. Bardeen and W. Press, J. Math. Phys. **14**, 7 (1973).

[17] S. Chandrasekhar, *The Mathematical Theory of Black Holes* (Oxford University Press, Oxford, England, 1983).

[18] I. Novikov and V. Frolov, *Physics of Black Holes* (Kluwer Academic, Dordrecht, Netherlands, 1989), pp. 194–195.

[19] William Krivan, Pablo Laguna, Philippos Papadopoulos, and Nils Andersson, Phys. Rev. D **56**, 3395 (1997).

[20] Manuela Campanelli, William Krivan, and Carlos O. Lousto, Phys. Rev. D **58**, 024016 (1998).

[21] Manuela Campanelli and Carlos O. Lousto, Phys. Rev. D **58**, 024015 (1998).

[22] Manuela Campanelli, Carlos O. Lousto, John Baker, Gaurav Khanna, and Jorge Pullin, Phys. Rev. D **58**, 084019 (1998).

[23] Manuela Campanelli and Carlos O. Lousto, Phys. Rev. D **59**, 124022 (1999).

[24] H. Bondi, M. van der Burg, and A. Metzner, Proc. R. Soc. London **A269**, 21 (1962).

[25] W. Israel, Phys. Rev. **143**, 1016 (1966).

[26] E. Newman and R. Penrose, J. Math. Phys. **3**, 566 (1962).

[27] C. Misner, Phys. Rev. **118**, 1110 (1960).

[28] I. Robinson and A. Trautman, Proc. R. Soc. London **A265**, 463 (1962).

[29] L. Derry, R. Isaacson, and J. Winicour, Phys. Rev. **183**, 1647 (1969).

[30] R. Gómez, R. L. Marsa, and J. Winicour, Phys. Rev. D **56**, 6310 (1997).

[31] Sascha Husa and Jeffrey Winicour, Phys. Rev. D **60**, 084019 (1999).

[32] Roberto Gómez, Sascha Husa, and Jeffrey Winicour, ''Complete null data for a black hole collision,'' Phys. Rev. D (to be published), gr-qc/0009092.

[33] David Garfinkle, Phys. Rev. D **51**, 5558 (1995).

[34] Hans-Peter Nollert and Bernd G. Schmidt, Phys. Rev. D **45**, 2617 (1992).

[35] Richard H. Price, Phys. Rev. D **5**, 2419 (1972).

[36] K. D. Kokkotas and B. G. Schmidt, Living Reviews in Relativity, http://www.livingreviews.org/Articles/Volume2/1999-2kokkotas/ (1999).